Sums and Densities of Fully Coupled Anharmonic Vibrational States: A Comparison of Three Practical Methods

ARTICLE *in* THE JOURNAL OF PHYSICAL CHEMISTRY A · FEBRUARY 2010

Impact Factor: 2.69 · DOI: 10.1021/jp100132s · Source: PubMed

2 AUTHORS:

Thanh Lam Nguyen
University of Texas at Austin
72 PUBLICATIONS **1,382** CITATIONS
SEE PROFILE

John R. Barker
University of Michigan
171 PUBLICATIONS **5,945** CITATIONS
SEE PROFILE

Sums and Densities of Fully Coupled Anharmonic Vibrational States: A Comparison of Three Practical Methods

Thanh Lam Nguyen and John R. Barker*

Department of Atmospheric, Oceanic and Space Sciences, University of Michigan, Ann Arbor, Michigan 48109-2143

Received: January 6, 2010; Revised Manuscript Received: February 4, 2010

Three practical methods for computing sums and densities of states of fully coupled anharmonic vibrations are compared. All three methods are based on the standard perturbation theory expansion for the vibrational energy. The accuracy of the perturbation theory expansion is tested by comparisons with computed eigenvalues and/or experimental vibrational constants taken from the literature for three- and four-atom molecules. For a number of examples, it is shown that the X_{ij} terms in the perturbation theory expansion account for most of the anharmonicity, and the Y_{ijk} terms also make a small contribution; contributions from the Z_{ijkl} terms are insignificant. For molecules containing up to ~4 atoms, the sums and densities of states can be computed by using nested DO-loops, but this method becomes impractical for larger species. An efficient Monte Carlo method published previously is both accurate and practical for molecules containing 3−6 atoms but becomes too slow for larger species. The Wang−Landau algorithm is shown to be practical and reasonably accurate for molecules containing ~4 or more atoms, where the practical size limit (with a single computer processor) is currently on the order of perhaps 50 atoms. It is shown that the errors depend mostly on the average number of stochastic samples per energy bin. An automated version of the Wang−Landau algorithm is described. Also described are the effects of Fermi resonances and procedures for deperturbation of the anharmonicity coefficients. Computer codes based on all three algorithms are available from the authors and can also be downloaded freely from the Internet (http://aoss.engin.umich.edu/multiwell/).

Introduction

Densities of states are useful for computing partition functions and for statistical chemical kinetics theories, including the Rice, Ramsperger, Kassel, and Marcus (RRKM) theory of unimolecular reactions and microcanonical transition-state theory (TST).[1−5] According to RRKM theory, the specific rate constants, $k(E,J)$, for unimolecular dissociation, for example, are proportional to the ratio of the sum of states of the transition state divided by the density of states of the reactant, where both quantities depend on internal energy and angular momentum. Because the reactant has higher internal energy than the transition state (TS), relative to their respective zero-point energies, and both have the same angular momentum, the density of states for the reactant is affected much more by anharmonicity than is the sum of states for the TS. This effect usually results in a significant reduction of $k(E,J)$ when anharmonicity is considered.

Sums and densities of states are readily computed by using separable models in which every degree of freedom is assumed to be completely uncoupled from all of the others. For separable models, the available algorithms include the steepest-descent method,[2] the semiclassical Whitten−Rabinovitch (WR) approximation,[6] and the combined Beyer−Swinehart[7] and Stein−Rabinovitch[8] (BSSR) algorithm, which carries out "direct count" calculations extremely efficiently. Computer programs implementing these methods are freely available (for example, the WR and BSSR methods are provided in program DenSum in the MultiWell program suite[9,10]). The required input data, such as harmonic vibrational frequencies and rotational constants, are easily obtained using electronic structure software packages. Generally, the harmonic oscillator model is adequate at low internal energies, but at higher energies, both the total anharmonicity, which is comprised of the anharmonicity of the separable modes and intermode coupling, becomes increasingly important. Replacing harmonic oscillators with separable Morse oscillators improves the results somewhat, but the total anharmonicity is still underestimated because the intermode coupling terms (e.g., between stretching and bending modes) are neglected.

In all real molecules, the internal degrees of freedom (DOF) are anharmonic and nonseparable (fully coupled). Intermode coupling is responsible for the fast intramolecular vibrational energy redistribution (IVR), which is a central premise in RRKM theory.[1−5] The importance of anharmonicity and intermode coupling depends on the size and complexity of a molecule. For a given total internal energy, the effect of anharmonicity in a single separable mode tends to be greater in a small molecule because the energy per mode is so much greater than that in a large molecule. However, the number of intermode coupling terms is equal to the square of the number of DOF, and therefore large molecules are affected to a much greater extent by intermode coupling. In all cases, the magnitude of the effects depends on the specific molecules.

Only a few methods exist for computing sums and densities of states for nonseparable vibrations. In principle, fully anharmonic sums and densities of states can be obtained from the spectrum of eigenvalues computed using direct quantum eigenstate calculations. Such calculations have been carried out, for example, on H_2O,[11] HO_2,[12] O_3,[13] NO_2,[14] CH_2O,[15] and H_2O_2.[16] Full-dimensionality eigenstate calculations for larger molecules are extremely challenging because the full-dimensional potential

* To whom correspondence should be addressed. E-mail: jrbarker@umich.edu.

10.1021/jp100132s
Published on Web 02/19/2010

energy surfaces must be known. The same difficulties arise for Monte Carlo integration of phase space volumes.[17−19] For larger molecules, the contribution of anharmonicity can be estimated using reduced dimensionality.

A number of approximate models have been proposed for estimating anharmonic, nonseparable densities of states. These include sampling classical phase space[20] or inverting the partition function, which is the Laplace transform of the density of states.[2] The partition function can be estimated through the use of empirical or calculated thermodynamic data.[21,22] Another approach is to invert the short-time approximation to the complex-time partition function.[23]

Empirical models also provide a useful means for estimating the effects of anharmonicity. For example, Troe has described an empirical approach in which Morse oscillator anharmonicities of stretching modes and generalized empirical stretch−bend couplings are postulated.[24,25] Schmatz has adopted much of the Troe model and has applied it to a series of very large alkanes (up to $C_{60}H_{122}$).[26] In the empirical approach, coefficients for various chemical classes are determined empirically, and the predictions must be verified by comparisons with more sophisticated calculation techniques before the model can be used with confidence. Nonetheless, this approach provides a way to predict molecular anharmoncity quickly.

Anharmonic fully coupled sums and densities of states can be computed directly by using perturbation theory expansions for the rovibrational energies in nested DO-loops. This approach is simple, highly efficient, and accurate for very small molecules when the anharmonicity coefficients are known. For slightly larger molecules, efficient Monte Carlo integration has been shown to be effective.[27] Recently, Basire et al.[28] reported using the relatively new Wang−Landau algorithm[29] for computing the density of states of fully coupled naphthalene, which has 48 vibrational DOF. For these methods, knowledge of the complete potential energy surface is unnecessary. They only require anharmonicity coefficients, which can be obtained from experimental data, from vibrational eigenvalue calculations, or from second-order vibrational perturbation theory (VPT2).[30−34] VPT2 has been implemented in quantum chemistry software packages such as Gaussian[35] and Cfour.[36] This capability is exceptionally important because one can compute the quadratic X_{ij} coefficients of the perturbation theory expansion for any molecule of moderate size and no empirical calibrations are necessary. Of course, the accuracy of the quantum chemical method is important, but even relatively inexpensive methods are reported to produce accurate results.[37−41] A possible drawback, however, is that the number of anharmonicity coefficient terms needed to achieve reasonable accuracy in a perturbation theory expansion is unknown, especially when extrapolating to and above bond dissociation energies.

In the present paper, we compare methods for computing fully coupled anharmonic vibrational sums and densities of states, based on the perturbation expansion approach. We begin by describing three algorithms for computing the sums and densities of states, direct enumeration (DO-loops), Monte Carlo integration, and Wang−Landau. We then compare sums and densities of states computed with the perturbation theory expansion to benchmark values obtained from spectroscopic experiments and from eigenvalue calculations taken from the literature. The results show that the quadratic anharmonicity terms (X_{ij}) account for most of the total anharmonicity involving small-amplitude vibrations, and the cubic terms (Y_{ijk}) account for the rest. We then compare the three algorithms to each other and to the benchmarks in order to assess errors. The Wang−Landau[29] algorithm as implemented by Basire et al.[28] requires several empirical parameters. We investigate the parametrization and describe methods for automating the algorithm. We also give examples of how Fermi resonances affect the computed sums and densities of states and how anharmonicity affects computed RRKM rate constants. We also show how to compute the sums and densities of states for combined separable and nonseparable DOF. In the end, we present an efficient procedure for computing sums and densities of states for nonseparable anharmonic vibrations in small to moderately large molecules. All computer codes described in this paper are available from the authors and also can be freely downloaded from the MultiWell Website.[42]

Methodology

Perturbation Theory Expansions. For asymmetric top molecules, the vibrational energy level relative to the zero-point energy is given by the following perturbation theory expansion for the vibrational energy[30,31,43]

$$E_v = -E_z + \sum_{i=1}^{N} \omega_i\left(v_i + \frac{1}{2}\right) + \sum_{i=1}^{N}\sum_{j=i}^{N} X_{ij}\left(v_i + \frac{1}{2}\right)\left(v_j + \frac{1}{2}\right) + \sum_{i=1}^{N}\sum_{j=i}^{N}\sum_{k=j}^{N} Y_{ijk}\left(v_i + \frac{1}{2}\right)\left(v_j + \frac{1}{2}\right)\left(v_k + \frac{1}{2}\right) + \sum_{i=1}^{N}\sum_{j=i}^{N}\sum_{k=j}^{N}\sum_{l=k}^{N} Z_{ijkl}\left(v_i + \frac{1}{2}\right)\left(v_j + \frac{1}{2}\right)\left(v_k + \frac{1}{2}\right)\left(v_l + \frac{1}{2}\right) + ... \quad (1)$$

where ω_i is the harmonic oscillator frequency, X_{ij}, Y_{ijk}, and Z_{ijkl} are the anharmonicity constants, v_i is the vibrational quantum number, N is the number of vibrational modes, and E_z is the zero-point vibrational energy, which is obtained by setting all $v_i = 0$

$$E_z = \frac{1}{2}\sum_{i=1}^{N}\omega_i + \frac{1}{4}\sum_{i=1}^{N}\sum_{j=i}^{N} X_{ij} + \frac{1}{8}\sum_{i=1}^{N}\sum_{j=i}^{N}\sum_{k=j}^{N} Y_{ijk} + \frac{1}{16}\sum_{i=1}^{N}\sum_{j=i}^{N}\sum_{k=j}^{N}\sum_{l=k}^{N} Z_{ijkl} + ... \quad (2)$$

The array of harmonic frequencies ($\boldsymbol{\omega}$) and the matrices composed of the anharmonicity constants ($\mathbf{X}$, $\mathbf{Y}$, $\mathbf{Z}$) can be either obtained from experiment or computed directly from first principles, for example, by quantum chemistry software packages equipped with VPT2.

When all quantized vibrational energy levels are known, sums and densities of states can be counted exactly. From eq 1, all E_v can, in principle, be computed when all allowed values of v are known. Therefore, the problem reduces to finding all allowed values of v_i up to a given total internal energy. For a separable harmonic oscillator, all quantum numbers from $v = 0$ to $v = \infty$ are allowed. A Morse oscillator, however, can dissociate and has only a finite number of vibrational states ranging from $v = 0$ to v_{max}. The allowed quantum numbers therefore range from $v = 0$ to v_{max}. For a coupled set of anharmonic vibrations, the maximum quantum number allowed for the kth vibration, $v_{D,k}$, depends on the quantum numbers assigned for all other vibrations. When the state energies are described by a perturbation theory expansion containing only $\mathbf{X}$ (i.e., $\mathbf{Y}$ and $\mathbf{Z} = 0$), $v_{D,k}$ can be found analytically[27]

$$v_{D,k} = \left[-\frac{\omega_k + \sum_{j \neq i} X_{kj}\left(v_j + \frac{1}{2}\right)}{2X_{kk}} - \frac{1}{2} \right] \tag{3}$$

It must be remembered that $v_{D,k}$ depends on all of the other quantum numbers. When $X_{kk} < 0$, then $v_{D,k}$ is the quantum number for the highest bound level of the kth vibration, and the corresponding dissociation energy (relative to the zero point energy) of this vibrational mode is D_k

$$D_k = -\frac{\left(\omega_k + \sum_{j \neq k} X_{jk}\left(v_j + \frac{1}{2}\right)\right)^2}{4X_{kk}} - \left(\frac{1}{2}\omega_k + \sum_{j \neq k} \frac{1}{4} X_{jk}\right) \tag{4}$$

This dissociation energy corresponds to the energy at which E_v reaches a maximum as v_k is increased, that is, $(\partial E_v/\partial v_k) = 0$ at $v_k = v_{D,k}$.

While computing the sums of states from $E_v = 0$ to a maximum value $E_v = E_{\text{tot}}$, the range of allowed quantum numbers is further restricted. Suppose one proceeds by first starting with all quantum numbers set to 0 and then assigning quantum numbers one at a time. After assigning $k - 1$ quantum numbers and before assigning the kth, $v_k = 0$, and the remaining unassigned energy E_u is given by

$$E_u = E_{\text{tot}} - E_{v,k-1} \tag{5}$$

where $E_{v,k-1}$ is the vibrational energy E_v computed using the $k - 1$ quantum numbers already assigned. The range of possible quantum numbers for the kth oscillator is therefore $v_k = 0$ to $v_{\text{max},k}$, where $v_{\text{max},k}$ depends on the amount of unassigned energy

$$v_{\text{max},k} = v_{D,k} \qquad \text{for } E_u \geq D_k \tag{6a}$$

$$v_{\text{max},k} = v_{D,k}\left[1 - \sqrt{1 - \frac{E_u}{D_k}}\right] \qquad \text{for } E_u \leq D_k \tag{6b}$$

When the **Y** and/or **Z** higher-order anharmonicities are included in eq 1, an analytical solution for $v_{D,k}$ is not obtainable, and iterative calculations are necessary. In the present work, $v_{\text{max},k}$ is computed iteratively by increasing trial values of v_k by unit steps from 0 and monitoring $E_v(v_k)$ while all other quantum numbers (v_i, $i \neq k$) are held constant. The iterative procedure stops as soon as $E_v(v_k)$ becomes smaller than $E_v(v_k - 1)$. This decrease corresponds to passing the maximum where $(\partial E_v/\partial v_k) = 0$. For a state to be "bound" with respect to the kth degree of freedom, the derivative must be greater than 0 for the trial value of v_k, $(\partial E_v/\partial v_k) > 0$. This process is repeated by increasing v_k until the $(\partial E_v/\partial v_k) < 0$ for a trial value of v_k. The assignment of $v_{D,k}$ is then based on the sign of the first derivative $(\partial E_v/\partial v_k)$ at $(v_k - 1)$ (see Figure 1), which enables one to ensure that the state with $v_{D,k}$ is lower in energy than the classical maximum E_v. When $(\partial E_v/\partial v_k)$ is > 0 at $(v_k - 1)$, then $v_{D,k} = v_k - 1$; otherwise, $v_{D,k}$ is set equal to $(v_k - 2)$.

At energies above the dissociation limit, quasi-bound states exist, where the quantum number for every mode does not exceed the dissociation limit for that particular mode. Of course, if the energy is redistributed, dissociation can take place. For computing RRKM rate constants, quasi-bound states must be counted. Quasi-bound states are identified when the partial derivatives are $(\partial E_v/\partial v_i) > 0$ for all i. Therefore, after all quantum numbers $\{v_i\}$ have been assigned, the partial derivatives $\{\partial E_v/\partial v_i\}_{i=1,N}$ are computed, and the assigned $\{v_i\}$ is accepted if all elements are positive; otherwise, the state is rejected.

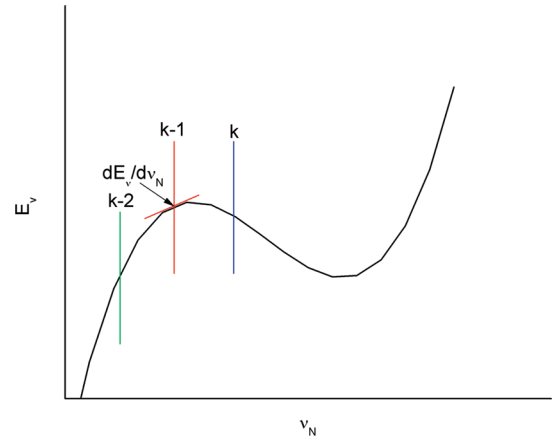

Figure 1. Vibrational energy level versus the unassigned v_N used to compute v_{max} according to the iterative method (see text).

Direct Counts. The direct count algorithm consists of straightforward nested DO-loops, which step through all allowed quantum numbers and compute E_v for all states up to a high energy (5×10^4 cm^{-1} in the present work). The energies are binned in energy grains of typically 10 cm^{-1}, and sums and densities of states can then be computed using the BSSR algorithm.[7,8] The number of nested DO-loops is equal to a number of DOF. The algorithm is very efficient for small molecules having 3−4 atoms but becomes extremely slow for larger species. A computer program entitled "doloops", which was written for computing direct counts, is available from the authors and can be freely downloaded from the MultiWell Website (http://aoss.engin.umich.edu/multiwell/).

Multidimensional Monte Carlo Integration. An efficient multidimensional Monte Carlo integration method has been described for computing sums of nonseparable vibrations.[27] In later developments, the method was extended to obtain total densities of states[44] and symmetry-specific densities of states.[45] In the present work, the original method, as implemented in computer program "ansum" (http://aoss.engin.umich.edu/multiwell/) was used to compute sums of states, $G_{\text{anh}}(E)$.

To reduce execution time, $G_{\text{anh}}(E)$ was calculated at fairly large energy intervals, even though a much smaller energy grain size was desired. Since the density of states is the derivative of the sum of states ($\rho(E) = \text{d}G/\text{d}E$), it is possible to obtain the density of states by fitting the computed $G_{\text{anh}}(E)$ to a suitable function and then taking the derivative. We instead chose to define an anharmonicity correction

$$F_G(E) = \frac{G_{\text{anh}}(E)}{G_h(E)} \tag{7}$$

where $G_h(E)$ is the sum of harmonic states, which we computed by using the Beyer−Swinehart algorithm as implemented in computer program DenSum[42] with a small energy grain size (typically 10 cm^{-1}). The density of harmonic states $\rho_h(E)$ was computed simultaneously. The anharmonicity correction $F_G(E)$ was fitted to a low-order polynomial. By rearranging eq 7 and taking the derivative, the anharmonic density of states was obtained

$$\rho_{anh}(E) = G_h(E) \times \frac{\partial F_G(E)}{\partial E} + \rho_h(E) \times F_G(E) \qquad (8)$$

Since $G_h(E)$ and $\rho_h(E)$ are computed with a small energy grain size, the anharmonic density of states $\rho_{anh}(E)$ is obtained with the same small energy grain.

The anharmonic correction factor for the density of states can be defined in a similar way

$$F_\rho(E) = \frac{\rho_{anh}(E)}{\rho_h(E)} = G_h(E) \times \frac{\partial F_G(E)}{\partial E} \times \left[\frac{\partial G_h(E)}{\partial E}\right]^{-1} + F_G(E) \qquad (9)$$

Since the first term on the right-hand side of eq 9 is always positive, $F_\rho(E)$ is always larger than $F_G(E)$. This can be seen for a series of alkanes in Table 3 of the paper by Schmatz.[26]

Wang−Landau Algorithm. Wang and Landau[29,46] pioneered an efficient random walk algorithm in energy space to compute densities of states for use in classical statistical models. Their approach is based on the idea that a density-weighted Monte Carlo sampling of the energy states of the system will produce a flat histogram of samples in equally spaced energy bins if the density of states function is exact, in the limit of an infinite number of trials. The algorithm is initiated with a trial density of states in every energy bin, and the density-weighted Monte Carlo sampling begins. A histogram records every visit to an energy bin. The algorithm is designed to modify the relative density of states $G(E_i)$ on every visit to an energy bin (at energy E_i) in such a way that $G(E_i)$ approaches exact proportionality with the true density of states after a large number of samples.[29,46] The algorithm can be halted by monitoring the "flatness" of the histogram or by limiting the number of Monte Carlo samples. Basire et al.[28] adapted the Wang−Landau algorithm for computing quantum densities of states for fully coupled anharmonic systems using the perturbation theory vibrational energy expression. It is a powerful method. For a full description of the algorithm and notation, see the paper by Basire et al.[28] As one of their demonstrations, they computed the density of states for naphthalene based on the fully coupled **X** matrix reported by Cané et al.[47]

We have modified the Basire et al. version[28] of the Wang−Landau algorithm in several minor ways to meet the needs for the density of states in chemical kinetics and master equation applications. In our approach, we compute statistics for the histogram based only on energy bins that contain states. We do not use the "flatness" criterion for halting the algorithm but instead use the number of Monte Carlo trials per energy bin since that is the principal factor that controls the relative error (see below). We also apply the tests described above to ensure that selected states are bound or quasi-bound.

We have automated the algorithm by choosing the probability of accepting a move (parameter p; see Basire et al. for notation) according to N, the number of DOF. As discussed by Basire et al., if p is too large, the Monte Carlo selection can sample the entire energy range rapidly, but there may be many wasted samples that fall out of range. On the other hand, if p is too small, the entire energy range may not be sampled efficiently, and more trials will be needed. In this work, we adopt $p = \mathrm{MIN}(1/N, 0.25)$. This protocol is consistent with the values for p used by Basire et al.[28] As discussed in a later section, our results show little sensitivity to the selection of p.

The most important new modification that we have made to the Basire et al. version[28] of the Wang−Landau algorithm is to introduce automatic normalization of the density of states. Recall that the Wang−Landau algorithm produces results that are proportional to the exact density of states. The un-normalized $G(E_i)$ may be sufficient for many applications, but the absolute density of states $\rho(E_i)$ is needed for calculating rate constants from statistical rate theories, for example. In our approach, the size of the energy bins (i.e., the energy grain size ΔE) is chosen small enough so that only one state, the lowest-energy state (i.e., the zero-point energy state), falls in the lowest-energy bin. Since we know that only one state resides in the lowest-energy bin, the density of states in the lowest-energy bin must be $(\Delta E)^{-1}$, and we then obtain the absolute density of states

$$\rho(E_i) = \frac{G(E_i)}{G(E_i = 0)} \frac{1}{\Delta E} \qquad (10)$$

For vibrational states, it is easy to choose ΔE small enough so that only the zero-point energy state falls within the lowest-energy bin. For master equation and chemical kinetics applications, the typical energy grain is $\Delta E \leq 10\ \mathrm{cm}^{-1}$, and vibrational frequencies are typically much larger. If rotations are to be included with the vibrations, normalization can still be achieved easily by using one of the other methods described above to count the number of rotational states in the lowest-energy grain and normalizing accordingly.

Our modified version of the Wang−Landau algorithm[29,46] draws heavily on that of Basire et al.[28] and is summarized as follows. For notation, see the paper by Basire et al.

Step 1: Set $g(E) = 0$ and $\ln(f) = 1$, where $g(E) = \ln(G(E_i))$; f is the modification factor, which is initially assigned to e^1.

Step 2: Initialize the set of vibrational quantum numbers $\{v_i\}_{old}$ randomly by Monte Carlo selection within the allowed space of quantum numbers and then compute the vibrational energy E_{old} using eq 1. Note that the computed results are almost independent of how the initial selections are made when the number of trials is large.

Step 3: Start the iteration loop for $I = 1$ to N_{iter}, which is the number of iterations. After each iteration, the value of f is reduced to $f_{new} = (f_{old})^{1/2}$. We use $N_{iter} = 21$ in order to achieve $f_{final} \approx 10^{-6}$. For larger N_{iter}, it is possible to achieve even greater accuracy, but only for an extraordinarily large number of trials. The increase of N_{iter} to 28, which corresponds to $f_{final} \approx 10^{-8}$, does not change the results in the first five significant digits, but the computational time is increased by ~35% for the same number of trials.

Step 4: Set $H(\mathrm{E}) = 0$, where $H(\mathrm{E})$ is the histogram, the number of stochastic trials visiting the energy bin at energy E.

Step 5: Start the second loop for $J = 1$ to N_{trial}, where N_{ttrial} is the total number of trials (i.e., Monte Carlo samples). The selection of N_{ttrial} will be discussed in the next section.

Step 6: Start the third loop for $K = 1$ to N, where N is the number of DOF.

Step 7: Compute a new set of quantum numbers $\{v_i\}_{new}$ by setting $p = \mathrm{MIN}(1/N, 0.25)$, and then compare a freshly generated unit deviate random number R_1 to p; if $R_1 \leq p$, assign $v_i = \mathrm{MAX}(0, v_i - 1)$; or if $p < R_1 \leq 2p$, assign $v_i = v_i + 1$; otherwise, do nothing.

Step 8: End the third loop.

Step 9: Use $\{v_i\}_{new}$ and eq 1 to compute and then check E_{new}. If E_{new} lies within the energy bound of interest (i.e., between $E_{min} = 0$ and E_{max}), go to step 10; otherwise, jump to step 13.

Step 10: If all first partial derivatives $\{\partial E_v/\partial v_i\}_{i=1,N}$ are positive, go to step 11; otherwise, jump to step 13. Note that this test was not considered in the work of Basire et al.

TABLE 1: Calculated Sums of Anharmonic States As a Function of Energy for H_2O, CH_2O, and CH_2D_2 Using Programs doloops (DL), ansum (AS)[a], and adensum (ADS)[b]

	H_2O			CH_2O			CH_2D_2		
E (cm^{-1})	DL	AS	ADS	DL	AS	ADS	DL	AS	ADS
1×10^4	23	23	23.03	631	630.2	631.7	4.120×10^3	4.098×10^3	4.126×10^3
2×10^4	130	130.8	130.4	1.508×10^4	1.512×10^4	1.507×10^4	2.914×10^5	2.883×10^5	2.923×10^5
3×10^4	434	432.8	435.4	1.286×10^5	1.278×10^5	1.285×10^5	5.522×10^6	5.555×10^6	5.542×10^6
4×10^4	1158	1157	1162	6.807×10^5	6.813×10^5	6.799×10^5		5.410×10^7	5.455×10^7
5×10^4	2721	2733	2729	2.796×10^6	2.795×10^6	2.794×10^6		3.592×10^8	3.629×10^8

[a] Thresholds: error = 0.5%, $N_{trials} = 2 \times 10^5$ per bin, and $\beta = 1.05$ (see Barker[27] for details). [b] Threshold = "BEST" with $N_{trials} = 10^5$ per bin (see text).

Step 11: If $\exp[g(E_{old}) - g(E_{new})] > R_2$ (a second unit deviate random number), go to step 12; otherwise, jump to step 13.

Step 12: Reset $\{v_i\}_{old} = \{v_i\}_{new}$ and $E_{old} = E_{new}$.

Step 13: Update $H(E_{old}) = H(E_{old}) + 1$ and $g(E_{old}) = g(E_{old}) + \ln(f)$,

Step 14: End the second loop.

Step 15: Reduce the modification factor f by reducing $\ln(f)$ by a factor of 2.

Step 16: End the first loop.

Step 17: Normalize to obtain the absolute density of states, $\rho(E) = \exp[g(E) - g(0)]/\Delta E$. Alternatively, by recognizing that the number of states in each energy grain is $\rho(E)\Delta E$, one can use the BSSR algorithm to carry out convolution with a collection of other DOF, not included with those considered so far. This enables one to convolute the densities of states for a collection of separable DOF with those for the coupled states that we are considering here and obtain the combined sum and density of states (see the next section).

This algorithm has been implemented in computer program "adensum" for computing fully coupled anharmonic sums and densities of states. With this computer program, densities of states for separable DOF can be convoluted with the anharmonic densities of states, as described in the next section.

Convolution with Separable DOF. Nonseparable DOF can be treated using the three methods described above. Except for the three DOF describing the center of mass, all molecular DOF are coupled. However, it is often the case that certain DOF are approximately separable, or the couplings are not well-understood. It is therefore convenient to treat some DOF as separable and others as coupled. The treatment of H_2O_2 in the JANAF Tables,[48] for example, consists of considering the small-amplitude bending and stretching vibrations as coupled among themselves but separable from the large-amplitude hindered internal rotation around the O−O bond. For all molecules, the "external" molecular rotations are coupled to vibrations and internal rotations, but, for convenience, the coupling is often neglected. It is therefore very useful to convolve the anharmonic densities of states computed by the methods described above with densities of states computed for separable DOF.

Convolution is readily achieved by using the Beyer−Swinehart algorithm[7] initialized with the density of states previously computed by one of the above methods. This approach was first described by Astholz et al.,[49] who convolved separable rotational and vibrational densities of states. Computer programs adensum, doloops, and ansum include the capability to convolute separable rotations (one-, two-, and three-dimensional) and one-dimensional hindered internal rotations. The treatment of hindered internal rotation employs the same implementation used in computer programs DenSum and Thermo (see the MultiWell user manual[42]), in which the hindered rotor eigenstates are computed numerically and then convolved with the other DOF.

TABLE 2: Comparison of Execution Time on a 64-Bit INTEL Node (two processors with 2 GB RAM each) Using Four Different Programs For H_2O, H_2O_2, CH_2O, CH_2D_2, and C_2H_6 for a Ceiling Energy of 5×10^4 cm^{-1} and a Grain Size of 10 cm^{-1}, unless Mentioned Otherwise

molecule	DenSum[a]	doloops	ansum[b]	adensum[c]
H_2O	<0.01 s	0.057 s	44.5 s	4.8 min
H_2O_2	<0.01 s	4.7 min	20.4 min	9.1 min
CH_2O	<0.01 s	92.0 min	70.3 min	9.2 min
CH_2D_2	<0.01 s		298.5 min[d]	16.0 min
C_2H_6	<0.01 s			47.0 min

[a] BSSR algorithm for separable DOF.[9,42] [b] Conditions: $N_{trials} = 10^7$ trials at each energy, nominal statistical error = 1%, and $\beta = 1.05$. [c] Conditions: N_{trials} per bin = 10^4 (keyword = "BETTER") and $p = 1/N_{DOF}$ (see text). [d] Using a grain (bin) size of 100 cm^{-1}. The computational time is 2901.3 min when a bin size of 10 cm^{-1} is used.

Results and Discussion

Algorithm Relative Performance. To compare the performance of the three algorithms, we computed anharmonic sums of states as a function of internal energy up to 5×10^4 cm^{-1} (10 cm^{-1} energy bins) for H_2O, CH_2O, and CH_2D_2. The results are presented in Table 1. Exact count results are not available for CH_2D_2 at the energies of $4-5 \times 10^4$ cm^{-1} because the calculations are too time-consuming. Table 1 shows that all three algorithms give results that agree within a statistical error of ~0.5%. The computational times are displayed in Table 2. The Densum computer program, which employs the BSSR algorithm for separable DOF, is much faster than the other methods, but it cannot deal with intermode coupling. On the basis of the computational time and accuracy for the fully coupled models, the doloops is the best choice for molecules having 3−4 atoms. The program ansum also works well for molecules with ≤6 atoms. Theoretically, adensum can be used with molecules of any size, but experience shows that it is the best choice for molecules with ≥4 atoms; the upper size limit is dictated by computer resources.

Accuracy of the Perturbation Theory Expansion. To determine the accuracy of the perturbation theory expansion for calculating sums and densities of states, the results were compared with literature data obtained from either quantum eigenstate calculations or spectroscopic measurements. Complete sets of eigenstates up to the dissociation threshold (D_0) are known for only a few small molecules. The accuracy of computed eigenstates depends on the potential energy surface and on the numerical methods employed. For testing computer algorithms, it is necessary to use anharmonicity coefficient matrices (**X**, **Y**, and **Z**) that are consistent with the computed eigenstates, but the level of agreement between experimental and computed eigenstates is not important; model calculations are good enough. In the following, we consider realistic (but

TABLE 3: Calculated Anharmonic Sums of States As a Function of Energy up to the H−O_2 Bond Dissociation Energy For $HO_2(X^2A')$[a]

energy (cm^{-1})	X matrix[b]	XY matrix[b]	eigenstates[c]
2×10^3	3	3	3
4×10^3	10	10	10
6×10^3	23	23	23
8×10^3	45	46	46
10×10^3	75	77	77
12×10^3	121	124	123
14×10^3	181	190	189
16×10^3	263	280	277
17×10^3	314	331	

[a] The results from eigenstate calculations are given for comparison. [b] Vibrational parameters were taken from Xu et al.[12] [c] From Xu et al.[12]

TABLE 4: Calculated Anharmonic Sums of States as a Function of Energy for $O_3(X^1A_1)$[a]

energy (cm^{-1})	X matrix[b]	XY matrix[b]	eigenstates[c]
2×10^3	7	7	7
4×10^3	33	33	33
6×10^3	93	94	94
7.5×10^3	167	171	175
8×10^3	198	205	
10×10^3	372	393	
12×10^3	645	701	
14×10^3	1042	1204	

[a] The results from eigenstates calculations are given for comparison. [b] Vibrational parameters were taken from Barbe et al.[50] [c] From Siebert et al.[13]

TABLE 5: Calculated Anharmonic Sums of States as a Function of Energy for $NO_2(X^2A_1)$ along with the Results from an Eigenstate Calculation Given for Comparison

energy (cm^{-1})	X matrix[a]	XYmatrix[a]	XYZ matrix[a]	eigenstates[b]
2×10^3	5	5	5	5
4×10^3	21	21	21	21
6×10^3	52	52	52	52
8×10^3	105	105	106	105
10×10^3	188	191	190	191
12×10^3	311	316	315	
15×10^3	578	601	596	
20×10^3	1359	1474	1438	
25×10^3	2754	3249	3041	

[a] Vibrational parameters were taken from Delon and Jost.[14] [b] From Delon and Jost.[14]

TABLE 6: Calculated Anharmonic Sums of States as a Function of Energy for $H_2O(X^1A_1)$[a]

	X matrix			eigenstates
energy (cm^{-1})	this work	T. J. Lee[b]	exptl.[c]	Li et al.[d]
5.0×10^3	6	6	6	6
1.0×10^4	23	23	23	23
1.5×10^4	62	62	62	64
2.0×10^4	132	130	130	134
2.5×10^4	256	255	256	246
3.0×10^4	442	440	434	416
3.5×10^4	736	730	714	670
3.981×10^4	1172	1169	1131	1053
4.0×10^4	1193	1192	1158	

[a] The results from eigenstate calculations are given for comparison. [b] From Huang-Lee.[53] [c] From Benedict.[52] [d] From Li et al.[11]

perhaps not perfect) models for HO_2, O_3, NO_2, and H_2O. Three types of calculations were carried out, using only the **X** matrix (labeled X), using the **X** and **Y** matrices (labeled XY), and using the **X**, **Y**, and **Z** matrices (labeled XYZ). The DO-loops algorithm was used in all cases.

For HO_2, computed eigenstates were taken from the work of Guo and co-workers,[12] who employed a high-quality potential energy surface at the icMRCI+Q/aug-cc-pVQZ level of theory. The calculated sums of states presented in Table 3 are in excellent agreement with those reported by Guo up to the energy of 1.6×10^4 cm^{-1} above the zero-point energy. The XY calculations produce results slightly better than those from the X calculations. However, even at $D_0 \approx 1.7 \times 10^4$ cm^{-1}, the difference between the two is only ~5%.

For O_3, the harmonic frequencies and the **X** and **Y** matrices were taken from the experimental work of Barbe and co-workers,[50] while the set of eigenstates was calculated by Siebert et al.[13] The calculated sums of states in Table 4 again show only a small difference between results obtained from the XY calculation and those obtained by the X calculation. Near the dissociation energy $D_0 \approx 8.5 \times 10^3$ cm^{-1}, the difference is only ~3%. Both are in good agreement with the sum of the eigenstates computed by Siebert et al.

For NO_2, the harmonic frequencies and the **X**, **Y**, and **Z** matrices were taken from the experimental work of Delon and Jost,[14] who also reported a set of eigenstates. The calculated sums of states up to the dissociation energy of $\sim 2.5 \times 10^4$ cm^{-1} are presented in Table 5. Note that vibrational states for the first electronic excited state A^2B_2, which is located at about 10^4 cm^{-1} above the ground state X^2A_1 and is not included in the present analysis, can introduce perturbations and other effects above $\sim 10^4$ cm^{-1}. As can be seen in Table 5, the calculated sums of states agree well with the experiments and the set of eigenstates up to 10^4 cm^{-1}, where the experimental data are available. At low energies, the results obtained in XY and XYZ calculations are indistinguishable, although there are small differences at higher energies. Overall, the XY calculations are as good as the XYZ. The X calculations also perform well, resulting in an error of only ~9%, compared to the XYZ calculation.

For H_2O, the complete set of eigenstates up to the dissociation energy ($D_0 \approx 3.98 \times 10^4$ cm^{-1}) was computed by Li et al., who used the potential energy surface of Partridge et al.[51] The harmonic frequencies and **X** matrix were taken from measurements[52] and a recent theoretical calculation[53] carried out at the TQ5+rel+ACPF/QZ level of theory. The **Y** and **Z** matrices were not known. The calculated sums of states are given in Table 6. The results obtained using the two different **X** matrices are in excellent agreement with each other and with the eigenstates given by Huang and Lee[53] but are slightly higher than the experiment. The X calculations agree well with the eigenstates up to 2.5×10^4 cm^{-1}, and at the dissociation energy, the difference is ~10%.

We also studied H_2O_2 and CH_2O, whose eigenstates have been computed up to a few thousand cm^{-1}.[15,16] In this low-energy range, as expected, the results of the X calculations are in agreement with the eigenstates (see Tables S7 and S8 in Supporting Information).

Taken together, these results support the conclusion that calculations using the perturbation theory expansion with just the **X** matrix are reasonably accurate up to the dissociation energy, capturing ~90% of the anharmonicity. Calculations that also include the **Y** matrix capture essentially all of the anharmonicity. This conclusion is based on only a few small molecules but appears to be robust. If this conclusion is correct

for smaller molecules, it is also appropriate for larger molecules because the average excitation per DOF is lower in larger molecules at the same total energy, which tends to reduce the effects of anharmonicity.

Wang−Landau Algorithm Parameterization. Several parameters that are required for the Lang−Landau algorithm can affect both accuracy and execution speed. These include the multiplicative factor f, the number of iterations, and the probability p. Our goal is to be able to compute densities of states with relative errors less than ~1%. We have adopted the scheme for specifying f that was originally outlined by Wang and Landau and used by Basire et al.[28] At the end of each iteration, ln f is reduced by 1/2 for a total of 21 iterations. By trial and error, we found that additional iterations did not significantly improve accuracy and simply added computation time.

As described by Basire et al., the choice of probability p affects the performance of the algorithm. When p is large, the algorithm rapidly covers the entire range of energies, but it also reduces efficiency because the algorithm steps out of the range of interest more frequently. This problem is exacerbated as the number of DOF increases. When p is too small, sampling requires more computing time to achieve the same accuracy. Basire et al. argued that p should be smaller for larger molecules and reported results for individual molecules chosen in the range from 0.04 to 0.23.[28]

We investigated how the algorithm performance depends on p by using a fixed value of $N_{trial} = 10^5$ per energy bin (10 cm^{-1} bins in the energy range from 0 to 5×10^4 cm^{-1}) and computed sums and densities of states for CH_2O, CH_2D_2, C_2H_5D, and C_6H_6. The average relative error is defined for the entire set of bins

$$\sigma = \left\{ \frac{1}{N_{bin}} \sum_{i=1}^{N_{bin}} \left(\frac{W_i}{W_i^0} - 1 \right)^2 \right\}^{1/2} \qquad (11)$$

where N_{bin} is the number of energy bins, W_i is the density of states (ρ_i) or sum of states (G_i) for the ith energy bin, and W_i^0 is the corresponding reference value, which is obtained from exact eigenvalues, when available, or from calculations that have much smaller relative errors (i.e., performed with a very large number of trials). In the present work, only densities of states were used to compute the average relative error.

The results are shown in Figure 2. For CH_2O and CH_2D_2, the errors are nearly independent of the choice of p, whereas for C_2H_5D and C_6H_6, the errors depend only weakly on p. Our results also confirm the statement of Basire et al. that the errors tend to increase when p becomes too larger and too small.[28] Given that the errors are not very sensitive to p, a reasonable choice is $p = \mathrm{MIN}(1/N_{DOF}, 0.25)$ which we have adopted in program adensum in order to automate the algorithm.

Wang−Landau Statistical Errors and N_{trial}. A rigorous analysis of the errors associated with the Wang−Landau algorithm is complicated[54] and beyond the scope of this paper. However, qualitative considerations can provide the basis for some semiquantitative insights.

The first important source of error is a sampling error. The Wang−Landau algorithm uses a stochastic sampling technique based on a sampling frequency weighted by the inverse density of states. If the exact density of states is known, stochastic sampling will produce a flat sampling histogram, meaning that all energy bins will have been sampled the same number of times, within some range of error. If we consider a span of energy divided into a large number N_{bin} of bins, the probability of sampling any specific bin is small (i.e., $1/N_{bin}$) in a given trial. For a large number of trials, the sampling probability of a single bin will be described by a Poisson distribution with mean $\mu = N_{trial}$, the average number of samples per bin, and the average standard deviation is $\sigma = \mu^{1/2}$. Thus, the average relative error is $\sigma/\mu = N_{trial}^{-1/2}$. The total number of trials is the product $N_{bin}N_{trial}$. As the number of stochastic trials increases indefinitely, the relative error will approach 0. For a finite number of trials, this relative sampling error is finite and contributes to the average relative error.

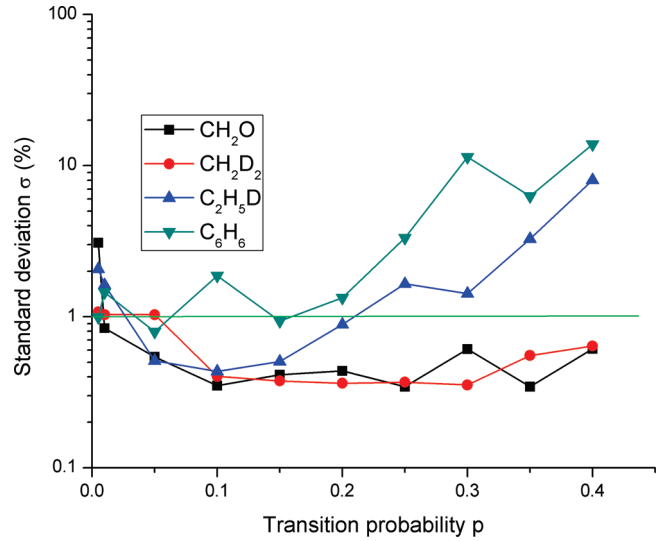

Figure 2. Relative errors in the densities of states as a function of transition probability p for CH_2O, CH_2D_2, C_2H_5D, and C_6H_6.

A second important source of error is associated with how the Wang−Landau algorithm starts with a trial density of states (assumed to be independent of energy) and ends with an estimate of the true density of states, which is a very strong function of energy. In pyrazine ($C_4H_4N_2$), a typical molecule of interest to our group, the density of vibrational states increases by ~18 powers of ten between its zero-point energy and its lowest dissociation energy. By using logarithms, the sheer magnitude of this numerical variation is reduced. By using multiplicative factors instead of simple linear sums, the convergence is accelerated. The algorithm can be envisioned as follows. In the first iteration, a large multiplicative factor (typically e^{+1}) is used to quickly obtain an order-of magnitude representation of the relative density of states. In subsequent iterations, in which the magnitude of the multiplicative factor is reduced, the sampling results in smoothing out the large fluctuations due to sampling errors in the first iteration. Of course, each subsequent iteration not only smooths the trial density of states but adds its own sampling fluctuations. The net result of these effects is to produce a good approximation to the relative density of states, which for some purposes must be normalized.

A third important source of error occurs when normalizing the relative density of states. Our approach is to use the known density of states in the lowest-energy bin for normalization, as described above. Since the histogram for this bin is, like all of the other bins, subject to sampling fluctuations, the sampling error in the first bin will affect the normalization factor. Considering that the sampling errors are expected to be proportional to $N_{trial}^{-1/2}$, we expect the total relative errors also to be roughly proportional to $N_{trial}^{-1/2}$.

To investigate the relative errors in the computed densities of states, we chose energy ranges and energy bin sizes that are

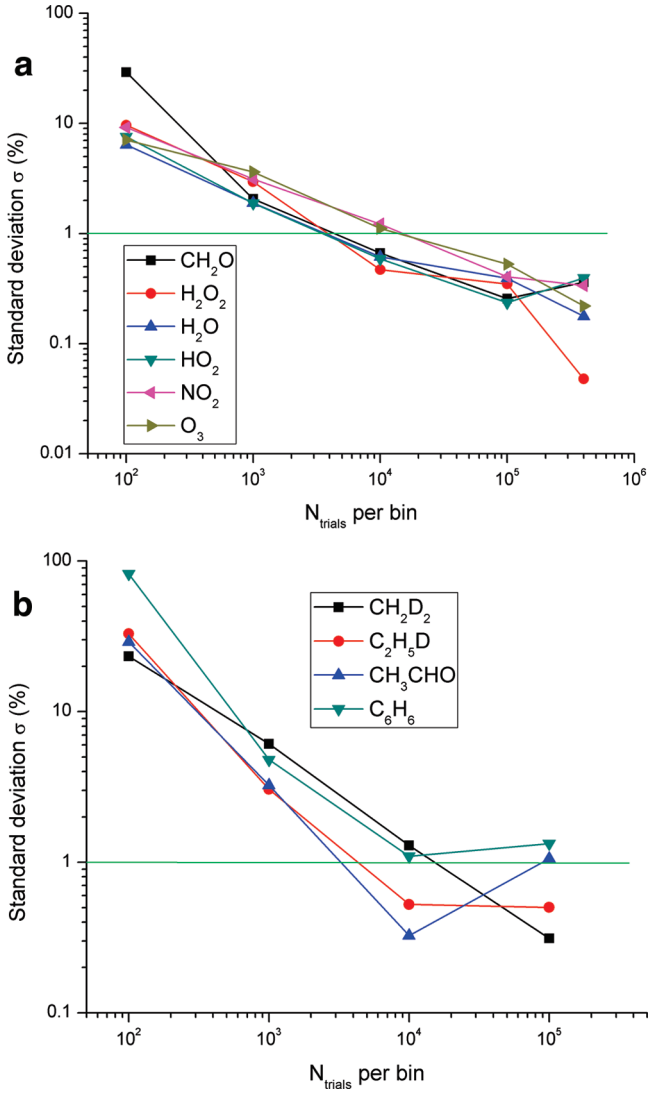

Figure 3. (a) Relative errors in the densities of states as a function of N_{trial} (trials per energy bin) for O_3, NO_2, HO_2, H_2O, H_2O_2, and CH_2O. (b) Relative errors in the densities of states as a function of N_{trial} (trials per energy bin) for CH_2D_2, C_2H_5D, CH_3CHO, and C_6H_6.

typical of master equation calculations for simulating atmospheric and combustion chemistry, bin sizes of 10 cm^{-1} and maximum vibrational energies of 5×10^4 cm^{-1}, corresponding to 5001 energy bins. Calculations were carried out using N_{trial} (per energy bin) = 10^2, 10^3, 10^4, 10^5, and 10^6, which are designated in the adensum computer program by the corresponding keywords, "FAIR", "GOOD", "BETTER", "BEST", and "EXTRA".

The results displayed in Figure 3a for six small molecules show that the relative errors are proportional to $N_{trial}^{-1/2}$, as anticipated. However, the results obtained for C_2H_5D, CH_3CHO, and C_6H_6 (see Figure 3b) show that the relative error is proportional to $N_{trial}^{-1/2}$ for relatively small N_{trial} but then approaches a constant value for $N_{trial} \approx 10^4-10^5$ trials per bin. This result is qualitatively similar to the result obtained by Lee et al.,[54] who applied the Wang−Landau algorithm to an Ising model. Calculations for H_2O, HO_2, O_3, NO_2, H_2O_2, and CH_2O are presented in the Supporting Information. In most cases, the "BETTER" option ($N_{trial} = 10^4$ trials/bin) is a good compromise between accuracy and execution time.

Computing the X Matrix. It is of interest to understand which methods are suitable to obtain harmonic frequencies and anharmonic constants for computing anharmonic densities of states using our programs in practice. The previous works of Martin, Lee, and Taylor[33,55−59] for a series of small-sized molecules show that the gold-standard method CCSD(T) in combination with a basis set cc-pVTZ can reproduce experimental harmonic and fundamental frequencies within 10 cm^{-1}. Given that a grain size of 10 cm^{-1} is frequently used in our simulations, the computed anharmonic densities of states using the CCSD(T)/cc-pVTZ data are nearly exact. However, the CCSD(T)/cc-pVTZ level of theory becomes so expensive in terms of computational time and the requirement of computer resources for anharmonic calculations, even for moderate-sized molecules. Alternative methods, which compensate between accuracy and computational time, are obviously needed. Recent studies by several groups[34,37−41] show the DFT-B3LYP method to be a good choice for such a circumstance. In this work, we chose the CH_2D_2 molecule as an example to compare three well-known methods involving CCSD(T), B3LYP, and MP2 with the experiment available. The computed anharmonic sums of states for CH_2D_2 relative to the experimental one[60] in Figure 4 using three different methods involving CCSD(T),[33] B3LYP, and MP2 support and confirm the above-mentioned results. As can be seen in Figure 4, the CCSD(T) values are very close to the experiment, next is B3LYP, and the worst is MP2. Overall, the averaged difference between B3LYP and the experiment is ~5%, whereas that of MP2 is ~20%. Until a systematic study of appropriate methods becomes accessible, we currently recommend using the B3LYP method for medium- to large-sized molecules and CCSD(T) for small ones to compute anharmonicity.

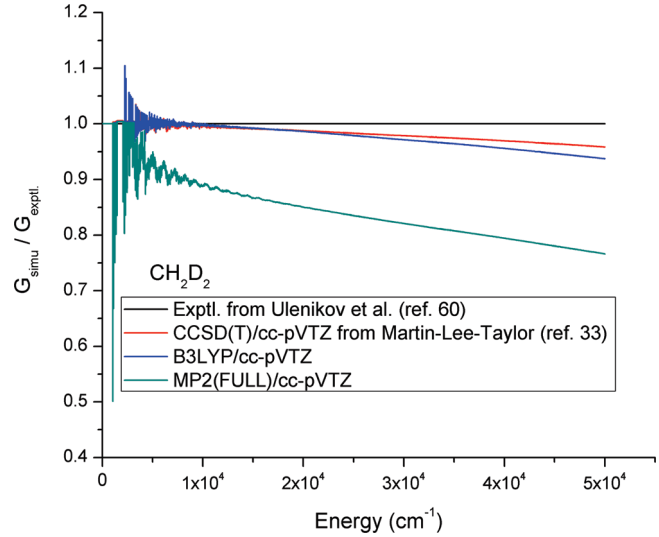

Figure 4. Anharmonic sums of vibrational states relative to that of experiment for CH_2D_2, computed at three different levels of theory.

Some Applications. In this section, we give some examples of the use of the program adensum for calculating anharmonic densities of states and how they affect predicted TST and RRKM reaction rates.

Methane and Ethane. Previously, Schmatz used a semiempirical method to compute anharmonic corrections $F_\rho(E)$ for CH_4 and C_2H_6 of 2.006 and 1.992, respectively, at the dissociation energies (36140 cm^{-1} for CH_4 and 30740 cm^{-1} for C_2H_6).[26]

Both CH_4 (T_d) and C_2H_6 (D_{3d}) are symmetric top molecules, which creates a problem in carrying out the vibrational analysis[34,61] and computing the **X** matrix. The standard implementations of vibrational perturbation theory used by the quantum chemical codes (and eq A3 and A4 in the Appendix) are valid only for asymmetric top molecules. For symmetric

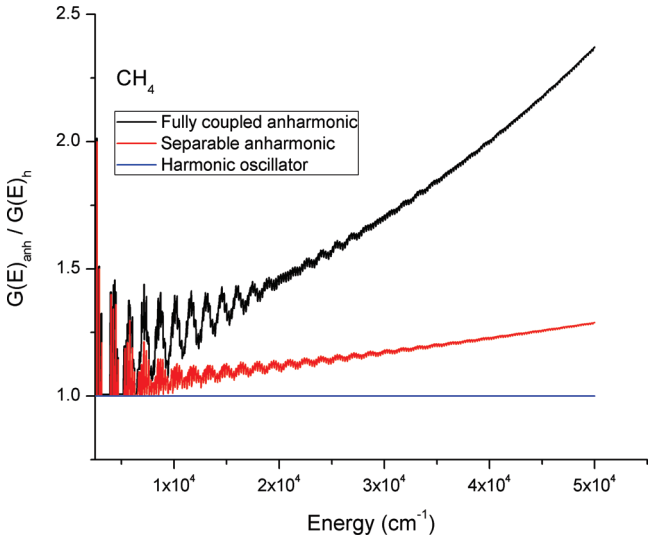

Figure 5. Ratio of anharmonic and harmonic sums of vibrational states for CH_4.

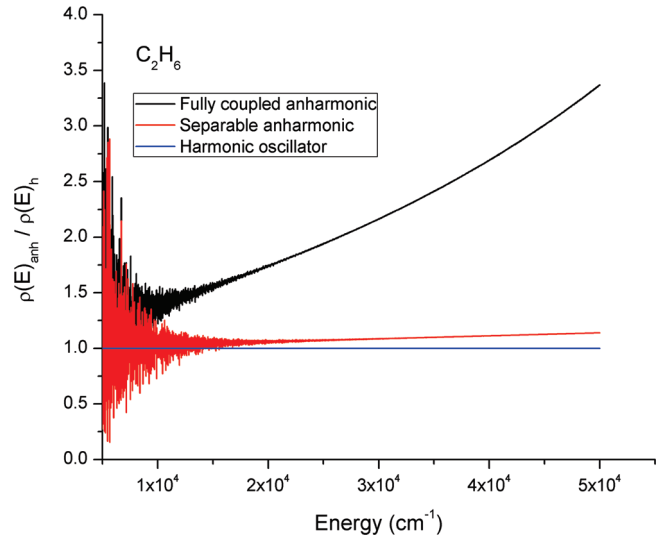

Figure 6. Ratio of anharmonic and harmonic densities of vibrational states for C_2H_6.

top molecules, these implementations fail to produce accurate results. A simple way to solve this problem is to change the masses of some of the atoms slightly in a symmetric top, just enough to destroy the symmetry but not enough to influence the computed frequencies significantly. For example, this method has been used to compute the vibrational anharmonicity of benzene by changing the carbon masses at the 1 and 4 positions from 12.000 to 12.002 amu.[61] The effect on the computed vibrational frequencies is ≤ 0.1 cm^{-1}.

In the present calculations for methane and ethane, the symmetries of the two molecules were reduced to C_{2v} and C_s, respectively, by changing the masses of two H atoms in CH_4 and one H atom in C_2H_6 from the nominal value of 1.00783 to 1.00001 amu, resulting in a change in the computed vibrational frequencies of ≤ 0.1 cm^{-1}. The harmonic frequencies and **X** matrices for both molecules were obtained at the B3LYP/cc-pVTZ level of theory with Opt=VeryTight and Int=UltraFine using Gaussian. In addition, the **X** matrices were deperturbed before use, as described in the Appendix. The deperturbation detected Fermi resonances by employing thresholds of 10 cm^{-1} for the cubic force constant and 100 cm^{-1} for the harmonic frequency difference (see Appendix for more details). The internal rotation around the C−C axis in C_2H_6 was separated from the other coupled vibrational motions and treated as a separable 1D-hindered internal rotor, as described above.

The computed anharmonic corrections $F_\rho(E)$ for CH_4 and C_2H_6 as a function of internal energy are plotted in Figures 5 and 6, respectively. For comparison, a model consisting of separable Morse oscillators is also presented. The figures show that for both separable and nonseparable models, the anharmonic contributions are scattered at low energy and increase at higher energies. The separable model recovers only a little of the anharmonicity because the bend−stretch coupling, which is very important in alkanes,[24,26] is neglected. At the bond dissociation energies, the fully coupled model predicts anharmonic corrections of 1.87 and 2.20 for CH_4 and C_2H_6, respectively, which are in reasonable agreement with the values obtained semiempirically by Schmatz.[26]

Naphthalene ($C_{10}H_8$). The anharmonic corrections for naphthalene ($C_{10}H_8$) were computed for comparison with the results reported by Basire et al.,[28] which were also obtained using the Wang−Landau algorithm. All vibrational data were taken from the published work of Cane et al.[47] The calculation with program adensum (with the "BETTER" option) required 5.6 h using a 64-bit INTEL CPU node (two processors, each with 2 GB RAM) for a ceiling energy of 5×10^4 cm^{-1} and a grain size of 10 cm^{-1}. With the "BEST" option, the computation time was 53.1 h. The results (Figure) show that the fully coupled anharmonicities are significant and increase nearly linearly with energy. The separable Morse oscillator model recovers only a negligible amount of the anharmonicities even at the highest energy. The results obtained using the "BEST" option are smoother and less scattered than those obtained using the "BETTER". These results are very similar to Figure 2 in Basire et al.[28] At 6 eV ($\sim 4.84 \times 10^4$ cm^{-1}), the present calculation gives $F_\rho(E) = 2.88$, close to the value of ~ 2.72 obtained by Basire et al., who employed a somewhat different parametrization for the Wang−Landau algorithm.

Reaction Rate Constants. One of the principal applications of sums and densities of states is to compute rate constants using statistical rate theories. The reaction step chosen for examination was the 1,4 H-shift isomerization of $CH_3C(=O)OO^\bullet$ to $^\bullet CH_2C(=O)OOH$, which is an important intermediate step in the reaction of acetyl radical with O_2.[62] The rovibrational parameters and barrier heights were taken from Maranzana et al.,[62] and the **X** matrix was computed at the B3LYP/6-311G(2df,p) level of theory. In $CH_3C(=O)OO^\bullet$, the internal rotors of the CH_3 group around the C−C axis and of the O_2 around the C−O axis were separated out from the other vibrations and treated as separable 1D-hindered internal rotors, according to the methods described above. As in Maranzana et al., tunneling corrections[63] were included by assuming an asymmetric Eckart potential. The high-pressure limit TST and RRKM rate calculations, which are displayed in Figures 8 and 9, respectively, show that the inclusion of anharmonicity results in significantly lower reaction rate constants, especially as the temperature or energy increases. As a result, the lifetime of the anharmonic reactant becomes longer and more pronounced at higher T or energy. These results are expected because the reactant has a much higher vibrational energy and the anharmonicity contributions are larger than those for TS. Figures 8 and 9 also show that the separable Morse oscillator model is inadequate, even near the reaction threshold.

Conclusions

In this work, three algorithms (and computer codes) for computing sums and densities of nonseparable anharmonic states

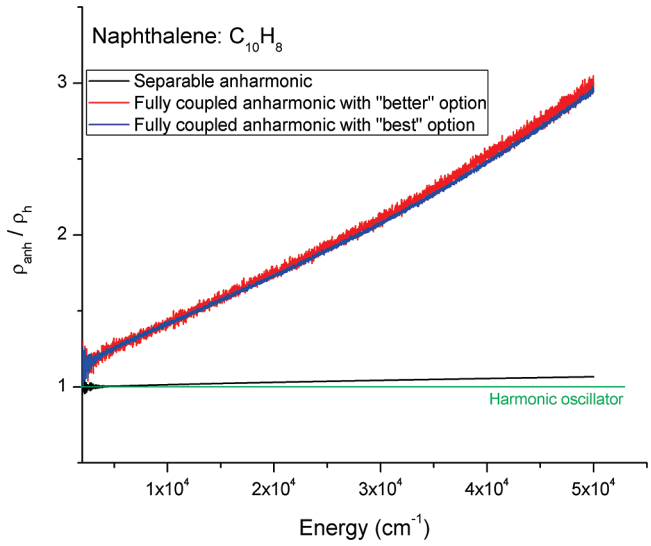

Figure 7. Ratio of anharmonic and harmonic densities of vibrational states for naphthalene $C_{10}H_8$.

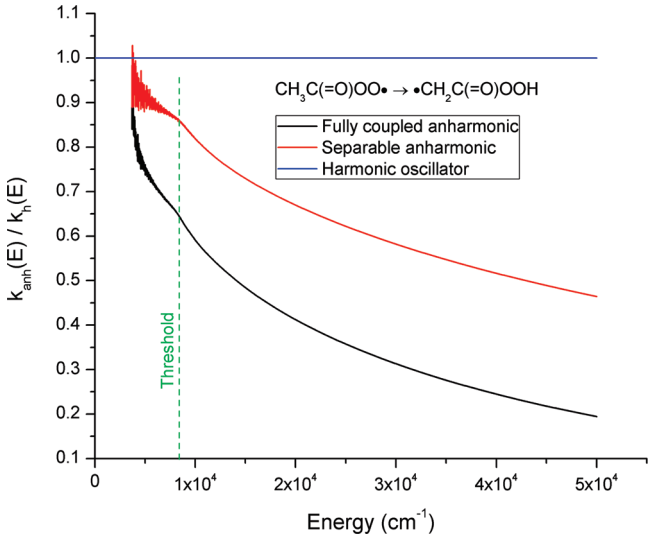

Figure 8. Ratio of anharmonic and harmonic RRKM reaction rate constants for the $CH_3C(=O)OO^{\bullet} \rightarrow {}^{\bullet}CH_2C(=O)OOH$ reaction channel as a function of internal energy.

are compared by carrying out calculations on molecules ranging from triatomics to napthalene ($C_{10}H_8$). The computed sums and densities of states are compared to the small set of available benchmarks, and the effects of anharmonicity on chemical reaction rate constants are illustrated. The following conclusions were reached.

- Perturbation theory expansions for eigenstate energies appear to be reasonably accurate up to the lowest dissociation energy and possibly above. Use of the **X** matrix by itself accounts for ~90% of the anharmonicity. Together, the **X** matrix and the **Y** matrix account for essentially all of the anharmonicity. The separable Morse oscillator model, which is commonly used with the Beyer−Swinehart/Stein−Rabinovitch approximation, is satisfactory only for small molecules at low energies; for large molecules at high energies, this model neglects the very important stretch−bend interactions and can account for only a small fraction of the total anharmonicity.
- Anharmonicities calculated using the three algorithms (DO-loops, Monte Carlo, and Wang−Landau and corresponding computer programs doloops, ansum, and adensum) agree among themselves and with direct eigenvalue calculations (taken from the literature) within 1%. Selection of the most efficient algorithm depends on the number of heavy atoms in the molecule; programs doloops and ansum are best for molecules with ≤4 atoms, and program adensum is best for the rest.
- The choice of the empirical parameters needed for efficient operation of the Wang−Landau algorithm has been automated for calculating sums and densities of anharmonic nonseparable molecular vibrations (program adensum).
- It is shown that densities of states from the coupled DOF can be readily convolved with those from separable DOF (like free rotations or hindered internal rotations) through use of the Beyer−Swinehart algorithm.
- The DFT-B3LYP level of theory with a moderately large basis set and appropriate settings for the calculation gives harmonic vibrational frequencies and X_{ij} anharmonicity coefficients that produce sums and densities of states in good agreement with those from eigenvalue calculations. The procedure for deperturbing the vibrational constants (i.e., removing the effects of Fermi resonances) is summarized in Appendix.
- Reaction rate constants calculated using statistical rate theories (e.g., RRKM, TST) are affected significantly by the anharmonicity of nonseparable DOF.

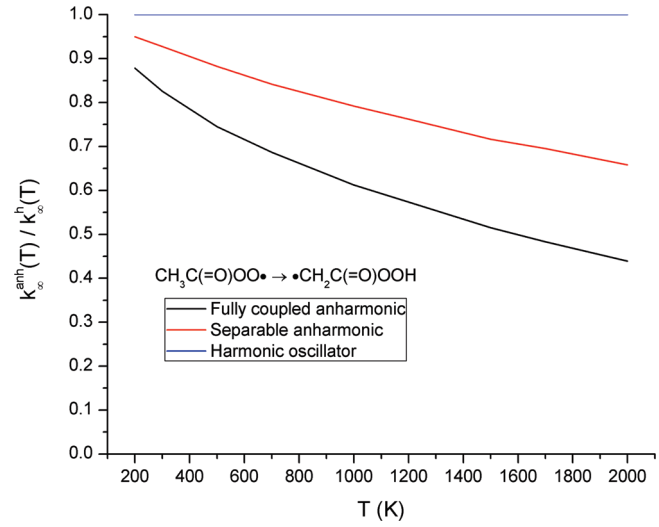

Figure 9. Ratio of anharmonic and harmonic TST reaction rate constants (i.e., high-pressure limit) for the $CH_3C(=O)OO^{\bullet} \rightarrow {}^{\bullet}CH_2C(=O)OOH$ reaction channel as a function of temperature.

It is also worth mentioning that the densities of anharmonic nonseparable states can be used easily to compute vibrational partition functions for large molecules. Although we have considered only the couplings associated with vibrational DOF, vibration−rotation interactions and other couplings can be included in a straightforward way. The standard thermodynamic properties can be derived from the partition function, including entropy, free energy, and heat capacity.

Acknowledgment. We thank the NSF (Atmospheric and Geospace Sciences) and NASA (Upper Atmosphere Research Program) for financial support. We are grateful to Anne B. McCoy for helpful conversations and for providing the results of her eigenvalue calculations. We also thank Yi Jie (Terrence) Chua, an undergraduate researcher, for helping with some preliminary calculations.

Appendix

Deperturbation of Vibrational Anharmonicity Constants. In this section, we discuss Fermi resonances and describe how to

compute an **X** matrix of "deperturbed" anharmonic vibrational constants using perturbation resonance theory.

According to second-order vibrational perturbation theory, the vibrational energy levels relative to the ground-state vibrational energy level of an asymmetric top molecule can be expressed as eq A1, that containing only the **X**-matrix of anharmonicity coefficients:[30,31]

$$E_v = \sum_{i=1}^{N} \omega_i\left(v_i + \frac{1}{2}\right) + \sum_{i=1}^{N}\sum_{j=i}^{N} X_{ij}\left(v_i + \frac{1}{2}\right)\left(v_j + \frac{1}{2}\right) - E_{0X} \tag{A1}$$

where ω is the harmonic oscillator frequency, N is the number of vibrational modes, v is the vibrational quantum number, and E_{0X} is the zero-point vibrational energy based on the **X** matrix

$$E_{0X} = \sum_{i=1}^{N} \omega_i/2 + \sum_{i=1}^{N}\sum_{j=i}^{N} X_{ij}/4 \tag{A2}$$

in which the vibrational anharmonicity constants X_{ij} (elements of the **X** matrix) can be obtained by using the following expressions[30−32,64]

$$X_{ii} = \frac{\phi_{iiii}}{16} - \sum_k \frac{\phi_{iik}^2}{32}\left(\frac{1}{2\omega_i + \omega_k} + \frac{4}{\omega_k} - \frac{1}{2\omega_i - \omega_k}\right) \tag{A3}$$

$$X_{ij} = \frac{\phi_{iijj}}{4} - \sum_k \frac{\phi_{iik}\phi_{ijk}}{4\omega_k} + \sum_\alpha B_\alpha(\zeta_{ij}^\alpha)^2\left(\frac{\omega_i}{\omega_j} + \frac{\omega_j}{\omega_i}\right) - \sum_k \frac{\phi_{ijk}^2}{8}\left(\frac{1}{\omega_i + \omega_j + \omega_k} + \frac{1}{-\omega_i + \omega_j + \omega_k} + \frac{1}{\omega_i - \omega_j + \omega_k} - \frac{1}{\omega_i + \omega_j - \omega_k}\right) \tag{A4}$$

in which ϕ_{ijk} and ϕ_{iijj} are the cubic and quartic force constants, respectively.[32,34,36,64,65] Because of the energy differences in the denominators, these expressions are strongly affected by Fermi resonances, where the perturbation approach fails.

There are two types of Fermi resonances

Fermi type 1 resonance: when $2\omega_i \approx \omega_k$ (near-degeneracy or $\Delta_1 = 2\omega_i - \omega_k \approx 0$)

Fermi type 2 resonance: when $\omega_i + \omega_j \approx \omega_k$ ($\Delta_2 = \omega_i + \omega_j - \omega_k \approx 0$).

When Fermi resonances exist, the denominators of some terms in eq A3 and A4 approach 0 (i.e., the terms become near-singular), resulting in "unusually large" magnitudes computed for some elements of **X**. The "deperturbation" approach[31,32,64] to this problem is to omit the near-singular terms in eq A3 and A4. The "deperturbed anharmonic constants" (X_{ii}* or X_{ij}*) are computed by excluding the near-singular terms and are usually denoted with an asterisk.[31,32,64] The relationships between X_{ii} and X_{ii}* and between X_{ij} and X_{ij}* are easily derived

Fermi type 1 resonance ($2\omega_i \approx \omega_k$):

$$X_{ii}^* = X_{ii} - \frac{\phi_{iik}^2}{32\Delta_1} \tag{A5a}$$

$$X_{ik}^* = X_{ik} + \frac{\phi_{iik}^2}{8\Delta_1} \tag{A5b}$$

where $\Delta_1 = 2\omega_i - \omega_k$.

Fermi type 2 resonance ($\omega_i + \omega_j \approx \omega_k$):

$$X_{ij}^* = X_{ij} - \frac{\phi_{ijk}^2}{8\Delta_2} \tag{A6a}$$

$$X_{ik}^* = X_{ik} + \frac{\phi_{ijk}^2}{8\Delta_2} \tag{A6b}$$

$$X_{jk}^* = X_{jk} + \frac{\phi_{ijk}^2}{8\Delta_2} \tag{A6c}$$

in which $\Delta_2 = \omega_i + \omega_j - \omega_k$.

Darling−Dennison[66] and Coriolis resonances must be considered when computing spectroscopic transitions, but their relatively small effects can be neglected when computing sums and densities of states. Darling−Dennison resonances shift overtone and/or combination fundamental frequencies by only a few wave numbers and do not affect the **X** matrix of anharmonic vibrational constants. Coriolis resonances influence the rotational but not the vibrational energies. They can be neglected as long as vibrations are assumed to be separable from rotations.

The current generation of quantum chemical software packages can compute anharmonic vibrational constants X_{ij} and X_{ij}*. For example, Gaussian03 deperturbs the **X** matrix by accounting for all Fermi resonances with the default criterion of $|\Delta| = 10$ cm^{-1} (here, the frequency difference Δ represents Δ_1 or Δ_2).[34,65] In contrast, CFOUR,[36] which is the successor of the Mainz−Austin−Budapest version of Aces-II,[67] uses the default of $|\Delta| = 50$ cm^{-1}. The most recent version of Gaussian (Gaussian09[68]) has again adopted the default criterion of $|\Delta| = 10$ cm^{-1} but allows the user to optionally select other values. Values for $|\Delta|$ ranging from 10 to 100 cm^{-1} can be found in the literature; there seems to be no firm consensus on how to select Fermi resonances for deperturbation.

To determine the influence of Fermi resonances on the computed sums and densities of states, we computed anharmonic corrections for CH_2O, CH_3CHO, CH_3OH, and C_6H_6 as a function of frequency difference Δ. All vibrational frequencies and anharmonicities were computed at the B3LYP/cc-pVTZ level of theory using Gaussian03. Note that anharmonicity calculations depend sensitively on optimized geometries computed at the previous job step; therefore, to obtain precise frequencies and anharmonic vibrational constants, the keyword OPT=VeryTight in the optimization step should be specified. In addition, for DFT calculations, the option INT=UltraFine should be included as well.[4] In computing the sums and densities of states, internal rotations were treated as 1D-hindered internal rotors and were assumed to be separable from the remaining vibrational modes. The results are shown in Figures S16−S19 (Supporting Information).

From Figures S16−S19 (Supporting Information), it is apparent that the computed sums and densities of states are not very sensitive to the value of Δ. Even for $\Delta = 500$ or 1000 cm^{-1}, the sums or densities are no more than ~10% different

from those obtained using $\Delta = 100$ cm^{-1}. The results for CH_4, C_2H_6, HCOOH, and H_2O_2, which are not presented here, show similar insensitivity to the magnitude of Δ. Thus, for pragmatic computation of sums and densities of states, we suggest that a value of $\Delta = 50$ or 100 cm^{-1} be used as the default.

Supporting Information Available: Harmonic frequencies, anharmonicity coefficients, and separable vibrational motions for various molecules are presented. Additionally, other results such as the effects of Fermi resonances are provided. This material is available free of charge via the Internet at http://pubs.acs.org.

References and Notes

(1) Robinson, P. J.; Holbrook, K. A. *Unimolecular Reactions*; Wiley-Interscience: London, New York, 1972.

(2) Forst, W. *Unimolecular Reactions. A Concise Introduction*; Cambridge University Press: Cambridge, U.K., 2003.

(3) Gilbert, R. G.; Smith, S. C. *Theory of Unimolecular and Recombination Reactions*; Blackwell Scientific: Oxford, U.K., 1990.

(4) Baer, T.; Hase, W. L. *Unimolecular Reaction Dynamics. Theory and Experiments*; Oxford University Press: New York, 1996.

(5) Holbrook, K. A.; Pilling, M. J.; Robertson, S. H. *Unimolecular Reactions*, 2nd ed.; Wiley: Chichester, U.K., 1996.

(6) Whitten, G. Z.; Rabinovitch, B. S. *J. Chem. Phys.* **1963**, *38*, 2466.

(7) Beyer, T.; Swinehart, D. F. *Commun. ACM* **1973**, *16*, 379.

(8) Stein, S. E.; Rabinovitch, B. S. *J. Chem. Phys.* **1973**, *58*, 2438.

(9) Barker, J. R. *Int. J. Chem. Kinetics* **2001**, *33*, 232.

(10) Barker, J. R. *Int. J. Chem. Kinetics* **2009**, *41*, 748.

(11) Li, G.; Guo, H. *J. Mol. Spectrosc.* **2001**, *210*, 90.

(12) Xu, C.; Jiang, B.; Xie, D.; Farantos, S. C.; Lin, S. Y.; Guo, H. *J. Phys. Chem. A* **2007**, *111*, 10353.

(13) Siebert, R.; Fleurat-Lessard, P.; Schinke, R.; Bittererova, M.; Farantos, S. C. *J. Chem. Phys.* **2002**, *116*, 9749.

(14) Delon, A.; Jost, R. *J. Chem. Phys.* **1991**, *95*, 5686.

(15) Burleigh, D. C.; McCoy, A. B.; Sibert, E. L., III. *J. Chem. Phys.* **1996**, *104*, 480.

(16) Ma, R. C. G.; Guo, H. *J. Chem. Phys.* **2001**, *114*, 4763.

(17) Berblinger, M.; Schlier, C. *J. Chem. Phys.* **1992**, *96*, 6834.

(18) Berblinger, M.; Schlier, C. *J. Chem. Phys.* **1992**, *96*, 6842.

(19) Taubmann, G.; Schmatz, S. *Phys. Chem. Chem. Phys.* **2001**, *3*, 2296.

(20) Ming, L.; Nordholm, S.; Schranz, H. W. *Chem. Phys. Lett.* **1996**, *248*, 228.

(21) Borjesson, L. E. B.; Nordholm, S.; Andersson, L. L. *Chem. Phys. Lett.* **1991**, *186*, 65.

(22) Krems, R.; Nordholm, S. *Z. Phys. Chem.* **2000**, *214*, 1467.

(23) Wadi, H.; Pollak, E. *J. Chem. Phys.* **1999**, *110*, 8246.

(24) Troe, *J. Chem. Phys.* **1995**, *190*, 381.

(25) Troe, J.; Ushakov, V. G. *J. Phys. Chem. A* **2009**, *113*, 3940.

(26) Schmatz, S. *Chem. Phys.* **2008**, *346*, 198.

(27) Barker, J. R. *J. Phys. Chem.* **1987**, *91*, 3849.

(28) Basire, M.; Parneix, P.; Calvo, F. *J. Chem. Phys.* **2008**, *129*, 081101.

(29) Wang, F.; Landau, D. P. *Phys. Rev. Lett.* **2001**, *86*, 2050.

(30) Nielsen, H. H. *Rev. Mod. Phys.* **1951**, *22*, 90.

(31) Mills, I. M. Vibration−Rotation Structure in Asymmetric- and Symmetric-Top Molecules. In *Molecular Spectroscopy: Modern Research*; Rao, K. N., Mathews, C. W., Eds.; Academic Press: New York, 1972; Vol. 1, p 115.

(32) Csaszar, A. G.; Mills, I. M. *Spectrochim. Acta, Part A* **1997**, *53*, 1101.

(33) Martin, J. M. L.; Lee, T. J.; Taylor, P. R. *J. Chem. Phys.* **1995**, *102*, 254.

(34) Barone, V. *J. Chem. Phys.* **2005**, *122*, 014108.

(35) Frisch, M. J.; Trucks, G. W.; Schlegel, H. B.; Scuseria, G. E.; Robb, M. A.; Cheeseman, J. R.; Montgomery, J. A., Jr.; Vreven, T.; Kudin, K. N.; Burant, J. C.; Millam, J. M.; Iyengar, S. S.; Tomasi, J.; Barone, V.; Mennucci, B.; Cossi, M.; Scalmani, G.; Rega, N.; Petersson, G. A.; Nakatsuji, H.; Hada, M.; Ehara, M.; Toyota, K.; Fukuda, R.; Hasegawa, J.; Ishida, M.; Nakajima, T.; Honda, Y.; Kitao, O.; Nakai, H.; Klene, M.; Li, X.; Knox, J. E.; Hratchian, H. P.; Cross, J. B.; Bakken, V.; Adamo, C.; Jaramillo, J.; Gomperts, R.; Stratmann, R. E.; Yazyev, O.; Austin, A. J.; Cammi, R.; Pomelli, C.; Ochterski, J. W.; Ayala, P. Y.; Morokuma, K.; Voth, G. A.; Salvador, P.; Dannenberg, J. J.; Zakrzewski, V. G.; Dapprich, S.; Daniels, A. D.; Strain, M. C.; Farkas, O.; Malick, D. K.; Rabuck, A. D.; Raghavachari, K.; Foresman, J. B.; Ortiz, J. V.; Cui, Q.; Baboul, A. G.; Clifford, S.; Cioslowski, J.; Stefanov, B. B.; Liu, G.; Liashenko, A.; Piskorz, P.; Komaromi, I.; Martin, R. L.; Fox, D. J.; Keith, T.; Al-Laham, M. A.; Peng, C. Y.; Nanayakkara, A.; Challacombe, M.; Gill, P. M. W.; Johnson, B.; Chen, W.; Wong, M. W.; Gonzalez, C.; Pople, J. A. Gaussian 03, revision C.02; Gaussian, Inc.: Wallingford, CT, 2004.

(36) *CFOUR*, a quantum chemical program package; Stanton, J. F.; Gauss, J.; Harding, M. E.; Szalay, P. G. with contributions from Auer, A. A.; Bartlett, R. J.; Benedikt, U.; Berger, C.; Bernholdt, D. E.; Bomble, Y. J.; Christiansen, O.; Heckert, M.; Heun, O.; Huber, C.; Jagau, T.-C.; Jonsson, D.; Jusélius, J.; Klein, K.; Lauderdale, W. J.; Matthews, D. A.; Metzroth, T.; O'Neill, D. P.; Price, D. R.; Prochnow, E.; Ruud, K.; Schiffmann, F.; Stopkowicz, S.; Tajti, A.; Vázquez, J.; Wang, F.; Watts, J. D. and the integral packages *MOLECULE* (Almlöf, J.; Taylor, P. R.); *PROPS* (Taylor, P. R.); *ABACUS* (Helgaker, T.; Jensen, H. A. Aa.; Jørgensen, P.; Olsen, J.); and *ECP routines* by Mitin, A. V.; van Wüllen, C. For the current version, see: http://www.cfour.de (2009).

(37) Carbonniere, P.; Lucca, T.; Pouchan, C.; Rega, N.; Barone, V. *J. Comput. Chem.* **2005**, *26*, 384.

(38) Miani, A.; Cane, E.; Palmieri, P.; Trombetti, A.; Handy, N. C. *J. Chem. Phys.* **2000**, *112*, 248.

(39) Neugebauer, J.; Hess, B. A. *J. Chem. Phys.* **2003**, *118*, 7215.

(40) Wang, J.; Hochstrasser, R. M. *J. Phys. Chem. B* **2006**, *110*, 3798.

(41) McKean, D. C.; Craig, N. C.; Law, M. M. *J. Phys. Chem. A* **2008**, *112*, 100006.

(42) Barker, J. R.; Ortiz, N. F.; Preses, J. M.; Lohr, L. L.; Maranzana, A.; Stimac, P. J.; Nguyen, T. L. MultiWell-2009.3 Software. http://aoss.engin.umich.edu/multiwell/ (2009).

(43) Herzberg, G. *Molecular Spectra and Molecular Structure. II. Infrared and Raman Spectra*, 2nd ed.; Van Nostrand Reinhold Co: Cincinnati, OH, 1945.

(44) Toselli, B. M.; Barker, J. R. *Chem. Phys. Lett.* **1989**, *159*, 499.

(45) Toselli, B. M.; Barker, J. R. *J. Phys. Chem.* **1989**, *93*, 6578.

(46) Wang, F.; Landau, D. P. *Phys. Rev. E* **2001**, *64*, 056101.

(47) Cané, E.; Miani, A.; Trombetti, A. *J. Phys. Chem. A* **2007**, *111*, 8218.

(48) Dorofeeva, O. V.; Iorish, V. S.; Novikov, V. P.; Neuman, D. B. *J. Phys. Chem. Ref. Data* **2003**, *32*, 879.

(49) Astholz, D. C.; Troe, J.; Wieters, W. *J. Chem. Phys.* **1979**, *70*, 5107.

(50) Barbe, A.; Chichery, A.; Cours, T.; Tyuterev, V. G.; Plateaux, J. J. *J. Mol. Struct.* **2002**, *616*, 55.

(51) Partridge, H.; Schwenke, D. W. *J. Chem. Phys.* **1997**, *106*, 4618.

(52) Benedict, W. S. *J. Chem. Phys.* **1956**, *24*, 1139.

(53) Huang, X.; Lee, T. J. *J. Chem. Phys.* **2008**, *129*, 044312.

(54) Lee, H. K.; Okabe, Y.; Landau, D. P. *Comput. Phys. Commun.* **2006**, *175*, 36.

(55) Martin, J. M. L.; Lee, T. J.; Taylor, P. R. *Chem. Phys. Lett.* **1993**, *205*, 535.

(56) Martin, J. M. L.; Lee, T. J.; Taylor, P. R. *J. Chem. Phys.* **1993**, *99*, 286.

(57) Martin, J. M. L.; Lee, T. J.; Taylor, P. R. *J. Mol. Spectrosc.* **1993**, *160*, 105.

(58) Martin, J. M. L.; Lee, T. J.; Taylor, P. R. *J. Chem. Phys.* **1992**, *97*, 8361.

(59) Martin, J. M. L.; Taylor, P. R. *Spectrochim. Acta, Part A* **1997**, *53*, 1039.

(60) Ulenikov, O. N.; Bekhtereva, E. S.; Albert, S.; Bauerecker, S.; Hollenstein, H.; Quack, M. *J. Phys. Chem. A* **2009**, *113*, 2218.

(61) Handy, N. C.; Willetts, A. *Spectrochim. Acta, Part A* **1997**, *53*, 1169.

(62) Maranzana, A.; Barker, J. R.; Tonachini, G. *Phys. Chem. Chem. Phys.* **2007**, *9*, 4129.

(63) Miller, W. H. *J. Am. Chem. Soc.* **1979**, *101*, 6810.

(64) Martin, J. M. L.; Lee, T. J.; Taylor, P. R.; Francois, J.-P. *J. Chem. Phys.* **1995**, *103*, 2589.

(65) Frisch, M. J.; Trucks, G. W.; Schlegel, H. B.; Scuseria, G. E.; Robb, M. A.; Cheeseman, J. R.; Montgomery, J. A., Jr.; Vreven, T.; Kudin, K. N.; Burant, J. C.; Millam, J. M.; Iyengar, S. S.; Tomasi, J.; Barone, V.; Mennucci, B.; Cossi, M.; Scalmani, G.; Rega, N.; Petersson, G. A.; Nakatsuji, H.; Hada, M.; Ehara, M.; Toyota, K.; Fukuda, R.; Hasegawa, J.; Ishida, M.; Nakajima, T.; Honda, Y.; Kitao, O.; Nakai, H.; Klene, M.; Li, X.; Knox, J. E.; Hratchian, H. P.; Cross, J. B.; Bakken, V.; Adamo, C.; Jaramillo, J.; Gomperts, R.; Stratmann, R. E.; Yazyev, O.; Austin, A. J.; Cammi, R.; Pomelli, C.; Ochterski, J. W.; Ayala, P. Y.; Morokuma, K.; Voth, G. A.; Salvador, P.; Dannenberg, J. J.; Zakrzewski, V. G.; Dapprich, S.; Daniels, A. D.; Strain, M. C.; Farkas, O.; Malick, D. K.; Rabuck, A. D.; Raghavachari, K.; Foresman, J. B.; Ortiz, J. V.; Cui, Q.; Baboul, A. G.; Clifford, S.; Cioslowski, J.; Stefanov, B. B.; Liu, G.; Liashenko, A.; Piskorz, P.; Komaromi, I.; Martin, R. L.; Fox, D. J.; Keith, T.; Al-Laham, M. A.; Peng, C. Y.; Nanayakkara, A.; Challacombe, M.; Gill, P. M. W.; Johnson, B.; Chen, W.; Wong, M. W.; Gonzalez, C.; Pople, J. A. Gaussian 03, revision C.02; Gaussian, Inc.: Wallingford, CT, 2004.

(66) Darling, B. T.; Dennison, D. M. *Phys. Rev.* **1940**, *57*, 128.

(67) Stanton, J. F.; Gauss, J.; Watts, J. D.; Szalay, P. G.; Bartlett, R. J.; Auer, A. A.; Bernholdt, D. B.; Christiansen, O.; Harding, M. E.; Heckert, M.; Heun, O.; Huber, C.; Jonsson, D.; Jusélius, J.; Lauderdale, W. J.;

Metzroth, T.; Michauk, C.; O'Neill, D. P.; Price, D. R.; Ruud, K.; Schiffmann, F.; Tajti, A.; Varner, M. E.; Vázquez, J.; Almlöf, J.; Taylor, P. R.; Helgaker, T.; Jensen, H. J. A.; Jørgensen, P.; Olsen, J. ACES2, a quantum-chemical program package for high-level calculations of energies and properties, Mainz−Austin−Budapest version. For the current version, see: http://www.aces2.de; Mainz-Austin-Budapest version ed (2006).

(68) Frisch, M. J.; Trucks, G. W.; Schlegel, H. B.; Scuseria, G. E.; Robb, M. A.; Cheeseman, J. R.; Montgomery J. A., Jr.; Vreven, T.; Kudin, K. N.; Burant, J. C.; Millam, J. M.; Iyengar, S. S.; Tomasi, J.; Barone, V.; Mennucci, B.; Cossi, M.; Scalmani, G.; Rega, N.; Petersson, G. A.; Nakatsuji, H.; Hada, M.; Ehara, M.; Toyota, K.; Fukuda, R.; Hasegawa, J.; Ishida, M.; Nakajima, T.; Honda, Y.; Kitao, O.; Nakai, H.; Klene, M.; Li, X.; Knox, J. E.; Hratchian, H. P.; Cross, J. B.; Bakken, V.; Adamo, C.; Jaramillo, J.; Gomperts, R.; Stratmann, R. E.; Yazyev, O.; Austin, A. J.; Cammi, R.; Pomelli, C.; Ochterski, J. W.; Ayala, P. Y.; Morokuma, K.; Voth, G. A.; Salvador, P.; Dannenberg, J. J.; Zakrzewski, V. G.; Dapprich, S.; Daniels, A. D.; Strain, M. C.; Farkas, O.; Malick, D. K.; Rabuck, A. D.; Raghavachari, K.; Foresman, J. B.; Ortiz, J. V.; Cui, Q.; Baboul, A. G.; Clifford, S.; Cioslowski, J.; Stefanov, B. B.; Liu, G.; Liashenko, A.; Piskorz, P.; Komaromi, I.; Martin, R. L.; Fox, D. J.; Keith, T.; Al.Laham, M. A.; Peng, C. Y.; Nanayakkara, A.; Challacombe, M.; Gill, P. M. W.; Johnson, B.; Chen, W.; Wong, M. W.; Gonzalez, C.; Pople, J. A. Cioslowski, J.; Fox, D. J. *Gaussian 09*, revision A.1; revision A.1; Gaussian, Inc: Wallingford CT, 2009.

JP100132S